Cosmic Ray Exposure Ages
Of Stony Meteorites:
Space Erosion
Or Yarkovsky?

by

David Parry Rubincam

Code 698

Planetary Geodynamics Laboratory

Solar System Exploration Division

NASA Goddard Space Flight Center

Building 34, Room S280

Greenbelt, MD 20771

voice: 301-614-6464

fax: 301-614-6522

email: David.P.Rubincam@nasa.gov

Abstract

Space erosion from dust impacts may set upper limits on the cosmic ray exposure (CRE) ages of stony meteorites. A meteoroid orbiting within the asteroid belt is bombarded by both cosmic rays and interplanetary dust particles. Galactic cosmic rays penetrate only the first few meters of the meteoroid; deeper regions are shielded. The dust particle impacts create tiny craters on the meteoroid's surface, wearing it away by space erosion (abrasion) at a particular rate. Hence a particular point inside a meteoroid accumulates cosmic ray products only until that point wears away, limiting CRE ages. The results would apply to other regolith-free surfaces in the solar system as well, so that abrasion may set upper CRE age limits which depend on the dusty environment. Calculations based on N. Divine's dust populations and on micrometeoroid cratering indicate that stony meteoroids in circular ecliptic orbits at 2 AU will record ^{21}Ne CRE ages of ~176 × 10^6 years if dust masses are in the range 10^{-21} – 10^{-3} kg. This is in broad agreement with the maximum observed CRE ages of ~100 × 10^6 years for stones. High erosion rates in the inner solar system may limit the CRE ages of Near-Earth Asteroids (NEAs) to ~120 × 10^6 years. If abrasion should prove to be ~6 times quicker than found here, then space erosion may be responsible for many of the measured CRE ages of main belt stony meteorites. In that case the CRE ages may not measure the drift time to the resonances due to the Yarkovsky effects as in the standard scenario, and that for some reason Yarkovsky is ineffective.

1. Introduction

The observed cosmic ray exposure (CRE) ages are typically ~1-100 × 10^6 years for stony meteorites, while iron meteorites have CRE ages on the order of ~600 × 10^6 years (e.g., McSween, 1999; Norton, 1994; Wood, 1968; Wieler and Graf, 2001). The usual explanation for the CRE ages of meteorites is catastrophic collision plus drift time plus resonance. In this scenario, a catastrophic collision between bodies in the asteroid belt creates fragments. Each fragment becomes a meteoroid. What are now fragments were mostly material buried so deeply in the parent bodies that they were shielded from galactic cosmic rays. The cosmic ray "clock" thus starts "ticking" once the fragments are exposed to the rays (e.g., Greenberg and Nolan, 1989).

The exposure continues while a meteoroid drifts to a resonance. The main mechanism for delivering meteoroids to the resonances is currently believed to be the Yarkovsky effects (e.g., Öpik, 1951; Peterson, 1976; Rubincam, 1987, 1995; Afonso et al., 1995; Bottke et al., 2000, 2002; Farinella and Vokrouhlicky, 1999). Irons drift slower than stones because their higher density and higher thermal conductivity lessen the Yarkovsky effects compared to stones, explaining their longer CRE ages.

In the Yarkovsky scenario, the drift time would mainly control a meteoroid's CRE age, since once it reaches a resonance, the meteoroid's orbital eccentricity is rapidly pumped up until its orbit crosses that of the Earth (Wisdom, 1983). The pumping timescale is only ~ a few 10^6 years (Gladman et al., 1997); so this part of the delivery process does not contribute much to the CRE age. Thereafter the meteoroid hits the Earth, to be picked up as a meteorite.

Two issues regarding meteoroid CRE ages are investigated here. The first issue is how space erosion by abrasion may at least place upper limits on stony meteorite CRE ages. The basic idea is illustrated in Fig. 1. Impacts from interplanetary dust excavate craters on a meteoroid, causing abrasion. Hence a meteoroid will slowly erode away over time.

However long that process takes sets an upper limit on the meteoroid's CRE age. Clearly no point inside the meteoroid can accumulate cosmic ray products once that point becomes the surface and erodes away. The first issue thus becomes: do the erosion upper limits do any violence to the measured CRE ages? If the erosion upper limits tended to be much shorter than the measured CRE ages, then there would be a problem. However, it is found that the erosion CRE ages are $> \sim 176 \times 10^6$ y for the assumed model for stony meteoroids originating in the main belt. This is in broad agreement with the measured CRE ages of $< \sim 100 \times 10^6$ y and allows the Yarkovsky drift timescale.

The second issue is whether space erosion may not just set maximum ages, but whether a better model might be reasonably expected to increase the erosion rate enough to lower the CRE ages into the observed range of many meteorites. If so, then CRE age may be decoupled from drift time. Stony meteoroids, for instance, could theoretically drift for very long periods of time before reaching a resonance, and still have CRE ages of (say) only $\sim 30 \times 10^6$ y. Certainly meteoroids can drift for extremely long stretches of time, because the iron meteoroids have characteristic CRE ages of $\sim 600 \times 10^6$ years. This leads to the provocative question: do CRE ages measure Yarkovsky drift times of stones at all? Perhaps Yarkovsky is weakened or inoperative for some reason and something slower causes the drift but still gives the observed CRE ages, thanks to space erosion.

On this second issue one can make arguments both for and against increasing the erosion rate found here (see section 6). Further investigation is indicated to see whether space erosion puts the Yarkovsky interpretation in jeopardy.

The present paper computes the rate of space erosion for stony meteoroids from dust impacts. Divine's (1993) interplanetary dust populations provide the impactors. Of his five distinct populations, only the core and asteroidal populations are used here. His eccentric, inclined, and halo populations make negligible contributions to abrasion and are ignored. Divine considers dust particles with masses in the range 10^{-21} kg - 10^{-3} kg; these limits are adopted here. The dust particles in his asteroidal population have typical masses of ~10^{-6} kg, corresponding to particle diameters of ~1 mm = 10^{-3} m. Some of Divine's (1993) velocity equations are derived in the Appendix as an aid to following his development.

The amount of mass excavated with each dust particle impact on a stony meteoroid is based on the work of Gault et al. (1972). The mass lost from the meteoroid by making these microcraters is typically many times the mass of the impacting particles.

Only the CRE ages derived from neon concentrations are examined here. The ^{21}Ne production rates are based on Eugster et al (2006).

In the following, the impacting particles are termed "dust", even though this includes particles up to 1 g = 0.001 kg, which is about the mass of the American dime coin (en.wiki.org/wiki/Dime_(United_States_coin)), the smallest coin of United States currency. The term "meteoroid" is reserved for the object hit by the dust.

Space erosion is an old topic (Whipple and Fireman, 1959; Fisher, 1961; Whipple, 1962; Schaeffer, 1981; Hughes, 1982; Wieler and Graf, 2001, p. 227, Welten et

al., 2001). The present paper focuses on space erosion by abrasion, and devotes only a few words to spallation.

Divine's (1993) elegant paper provides the conceptual framework for the present investigation; it is a fitting capstone to his career (Nunes, 1997). The mathematical treatment which follows differs only slightly from Divine's. Readers uninterested in the derivations can skip to Section 4.

2. Dust particle density

This section computes the number density of dust particles for the asteroidal and core populations. The result agrees with Divine (1993), giving confidence in the results that follow. The abrasion rate will be computed in the succeeding sections.

A dust particle's Cartesian position is given by

$$r\hat{\mathbf{r}} = x\hat{\mathbf{x}} + y\hat{\mathbf{y}} + z\hat{\mathbf{z}}, \tag{1}$$

where r is its distance from the Sun, $\hat{\mathbf{r}}$ is the unit position vector, and $\hat{\mathbf{x}}$, $\hat{\mathbf{y}}$, and $\hat{\mathbf{z}}$ are the unit vectors along the x, y, and z axes, respectively, where the z-axis is normal to the ecliptic. The dust particle is assumed to orbit the Sun in an ellipse, with the Keplerian orbital elements being (a, e, I, Ω, ω, M), where a is the semimajor axis, e is the orbital eccentricity, I is the orbital inclination to the ecliptic, and Ω is the nodal position. The other two Keplerian elements, argument of perihelion ω and mean anomaly M, will not be needed here. See Fig. 2 for the geometry of the orbit. Two auxiliary variables which

are used below are the perihelion distance $r_1 = a(1 - e)$ and the ecliptic latitude λ, where $\sin \lambda = z/r$. The unit vector $\hat{\mathbf{n}}$ normal to the dust particle's orbital plane is given by

$$\hat{\mathbf{n}} = (\sin I \sin \Omega)\hat{\mathbf{x}} - (\sin I \cos \Omega)\hat{\mathbf{y}} + (\cos I)\hat{\mathbf{z}} \ , \tag{2}$$

The notation above follows that of Divine (1993), apart from the substitution of I for his i and $(\hat{\mathbf{x}}, \hat{\mathbf{y}}, \hat{\mathbf{z}})$ for his $(\mathbf{u}_x, \mathbf{u}_y, \mathbf{u}_z)$.

The number density N_D of dust particles in units of number per cubic meter is given by:

$$N_D = \frac{H_D}{\pi} \int_0^r \frac{N_1 r_1}{r(r - r_1)^{1/2}} \, dr_1$$

$$\bullet \int_{\frac{r - r_1}{r + r_1}}^1 \frac{p_e}{[-(r - r_1) + (r + r_1)e]^{1/2}} \, de$$

$$\bullet \int_{|\lambda|}^{\pi - |\lambda|} \frac{p_I \sin I}{[(\cos^2 \lambda - \cos^2 I]^{1/2}} \, dI \quad . \tag{3}$$

This can be written more compactly as

$$N_D = \frac{H_D}{\pi} \int\int\int w(r_1, e, I) dr_1 de dI \tag{4}$$

to save space, where

$$w(r_1,e,I) = \frac{N_1 r_1}{r(r-r_1)^{1/2}} \frac{p_e}{[-(r-r_1)+(r+r_1)e]^{1/2}} \frac{p_I \sin I}{[\cos^2 \lambda - \cos^2 I]^{1/2}} \tag{5}$$

(Divine, 1993). In the above H_D is a cumulative number distribution

$$H_D = \int_{m_1}^{\infty} H_m \, dm_D \quad , \tag{6}$$

defined such that $H_D = 1$ for $m_1 = 1$ g $= 10^{-3}$ kg; H_m is a differential number distribution (Divine, 1993, p. 17,030).

In (3) p_I is a distribution which depends only on inclination I and p_e is a distribution which depends only on eccentricity e. Both the core and asteroidal populations have the same p_I and p_e. They follow the normalizations

$$\int_0^{\pi} p_I \, dI = 1 \tag{7}$$

$$\int_0^1 p_e \, de = 1 \quad . \tag{8}$$

As Matney and Kessler (1996) point out, though $p_e > 0$ and $p_I > 0$, they are not the "textbook" probability distributions; so that $p_e de$, for example, is not the number of objects between e and $e + de$. But as they also point out, Divine's p_I and p_e are internally consistent, and so will be used here. They are shown as the solid lines in Fig.s 3 and 4.

The integrals in (3) have to be evaluated. The first step in doing so is to express p_I and p_e in functions different from the straight lines in Fig.s 3 and 4, but still hew closely to their values. The new functions make the integrations over I and e in (3) more convenient.

The p_I distribution is the most easily dealt with. Divine (1993) writes it as a piecewise function of the form $c + bI$. Here p_I will instead be written piecewise in the form of $c + b \cos I$. This allows integrals of the form

$$\int_{|\lambda|}^{\pi-|\lambda|} \frac{\cos^n I \sin I}{[(\cos^2 \lambda - \cos^2 I]^{1/2}} dI \tag{9}$$

to be analytically evaluated by switching to the variable $\cos I$. The resulting expressions can be found from tables, such as given by Selby (1974, pp. 429). Table 1 gives the constants used for p_I; they are chosen so that the p_I used here closely resembles Divine's p_I, and obeys the normalization (7). Figure 3 compares the two functions. The agreement is good.

Divine similarly writes p_e as a piecewise function of the form $c + be$, but here it will be written as a continuous polynomial function of e on the interval [0,1]. The technique is as follows. First, the square root of Divine's piecewise function is written as a sum of Zernicke polynomials

$$p_e^{1/2} = \sum_{i=0}^{J/2} g_i Z_i(e) \tag{10}$$

where $Z_i(e)$ is the unnormalized Zernicke polynomial of order i and is summed to the finite value $J/2$. The Zernicke polynomials are orthogonal on [0,1] and are related to the Legendre polynomials (e.g., Beckmann 1973, pp. 150-156). The Zernicke polynomials are given by the equation

$$Z_i(e) = \sum_{k=0}^{i} \frac{(-1)^{i+k}(i+k)!}{(i-k)!(k!)^2} e^k \tag{11}$$

so that the first few polynomials are $Z_0(e) = 1, Z_1(e) = 2e - 1, Z_2(e) = 6e^2 - 6e + 1$, etc.

They have normalization

$$\overline{Z}_i(e) = (2i+1)^{1/2} Z_i(e) \tag{12}$$

so that

$$\int_0^1 [\overline{Z}_i(e)]^2 de = 1 \quad . \tag{13}$$

Also, in (10) the g_i are the unnormalized coefficients, given by

$$g_i = (2n+1) \int_0^1 p_e^{1/2} Z_i(e) de \tag{14}$$

where $p_e^{1/2}$ has the form $(c + be)^{1/2}$ where c and b piecewise have Divine's values. The equation (10) is then squared, resulting in an expression of the form

$$p_e = \sum_{j=0}^{J} A_j' e^j \quad . \tag{15}$$

The squaring guarantees that $p_e > 0$, as required. The integral becomes

$$\int_0^1 \sum_{j=0}^{J} A_j' \, e^j de = Q \quad . \tag{16}$$

The coefficients A_i' are then divided by Q, giving new coefficients $A_j = A_j'/Q$, so that

$$p_e = \sum_{j=0}^{J} A_j e^j \tag{17}$$

and (8) is satisfied. Figure 4 compares the continuous function (17) with Divine's piecewise function. The agreement is quite good. Table 2 gives the values for A_j.

Switching to the dimensionless variable $\xi = 2\{e - [(r - r_1)/ (r + r_1)]\}^{1/2}$, so that $e = [(r - r_1)/ (r + r_1)] + \xi^2/4$, avoids the singularity in the integral over e in (3). The integral can then easily be numerically integrated.

Finally, there is the integral over r_1 in (3) to be evaluated. Unlike p_I and p_e, the core and asteroidal populations have their own distinct N_1 functions, with the core N_1

function peaking close to the Sun and the asteroidal N_1 function peaking in the main belt (Fig. 5). Divine gives each N_1 distribution the piecewise form

$$N_1 = C r_1^{\alpha} \quad , \tag{18}$$

which is thus a function of r_1, with the constants C and α being given in Table 3. The problem in this case is that $(r - r_1)^{1/2}$ appears in the denominator, which leads to infinity problems when r_1 is close to r. This singularity in (3) in the integral over r_1 can be avoided by switching to the dimensionless variable $\zeta = [(r - r_1)/r]^{1/2}$, so that $r_1 = r\,(1 - \zeta^2)$. The resulting expression can easily be numerically integrated.

With the p_I, p_e, and N_1 in hand, N_D in (3) can be evaluated. Figure 6 shows N_D for the core and asteroidal populations as found by Divine (straight lines), while the dots are the N_D values computed here for distances between 0.5 AU and 5 AU. The agreement is quite good.

3. Space erosion due to dust particle impact abrasion

This section computes the rate of space erosion (abrasion) due to dust particle impacts on the meteoroid. It is first necessary to find the velocity of the dust and of the meteoroid, so that the relative velocity can be computed. From the relative velocity comes the kinetic energy which makes the craters.

Let **v** be the velocity of a dust particle in the inertial frame of Fig. 2. The dust particle's velocity is given by

$$\mathbf{v} = v_r \hat{\mathbf{r}} + v_{\phi}(\hat{\mathbf{n}} \times \hat{\mathbf{r}}) \tag{19}$$

where v_r is the radial speed, v_{ϕ} is the transverse speed, and $\hat{\mathbf{n}} \times \hat{\mathbf{r}}$ is the unit vector in the orbital plane transverse to $\hat{\mathbf{r}}$. The Cartesian velocities are given by Divine (1993):

$$v_x = (\mathbf{v} \cdot \hat{\mathbf{x}}) = \frac{x}{r} v_r - \left(\frac{r y v_{\phi} \cos I + x z v_s}{x^2 + y^2} \right) \ , \tag{20}$$

$$v_y = (\mathbf{v} \cdot \hat{\mathbf{y}}) = \frac{y}{r} v_r + \left(\frac{r x v_{\phi} \cos I - y z v_s}{x^2 + y^2} \right) \ , \tag{21}$$

and

$$v_z = (\mathbf{v} \cdot \hat{\mathbf{z}}) = \frac{z}{r} v_r + v_s \ , \tag{22}$$

where

$$v_r = \pm \left\{ \frac{G M_S}{r^2 r_1} (r - r_1)[-(r - r_1) + (r + r_1)e] \right\}^{1/2} \ , \tag{23}$$

$$v_{\phi} = + \left[\frac{G M_S r_1}{r^2} (1 + e) \right]^{1/2} \ , \tag{24}$$

and

$$v_s = \pm v_\phi (\cos^2 \lambda - \cos^2 I)^{1/2} \quad . \tag{25}$$

Here M_S is the mass of the Sun and G is the universal constant of gravitation. Divine (1993) presents these equations without giving the derivations; an outline of the derivations is given in the Appendix.

A collision occurs when the meteoroid's position and the dust particle's position coincide. In other words, when they have the same position $r\hat{\mathbf{r}}$ as given by (1). The collisions take place at the nodes of the dust particle's orbit.

Gault et al. (1972) find for polycrystalline rocks that the mass of material M_{ej} ejected from the surface of the meteoroid in an impact is given by $M_{ej} \approx 8.63 \times 10^{-11} E^{1.13} \cos^2 \Theta$, where E is the kinetic energy measured in ergs, M_{ej} is in grams, and Θ is the angle of the velocity vector with the local vertical. Converting Gault et al.'s equation to SI units gives

$$M_{ej} \approx K_{stone} [m_D (\Delta v)^2/2]^{1.13} \cos^2 \Theta \ , \tag{26}$$

where $K_{stone} = 7.015 \times 10^{-6}$, $E = m_D(\Delta v)^2/2$ is the kinetic energy and is now in joules, and m_D is the mass of the impacting dust particle in kg. Also, Δv is its speed relative to the meteoroid in m s^{-1}, where

$$(\Delta v)^2 = (\mathbf{v} - \mathbf{v}_M) \cdot (\mathbf{v} - \mathbf{v}_M) \ ,$$

with $\mathbf{v}_M$ being the velocity of the meteoroid.

To account for the oblique impacts embodied by $\cos^2 \Theta$, it will be reasonably assumed that the dust particles pelting the meteoroid from a particular direction will be spread uniformly over the circular cross-sectional area seen by the incoming particles. Considering the number of particles impacting an annulus of radius $R\sin \Theta$ and width $R\cos \Theta \, d\Theta$ (Fig. 7) and averaging over the hemisphere pelted by the dust gives

$$R^2 \int_0^{2\pi} \int_0^{\pi/2} \sin\Theta \cos\Theta \cos^2\Theta \, d\Theta \, d\Phi \, / \, R^2 \int_0^{2\pi} \int_0^{\pi/2} \sin\Theta \cos\Theta \, d\Theta \, d\Phi = 1/2 \qquad (27)$$

as the factor needed to find the average amount of ejected mass $<M_{ej}>$:

$$<M_{ej}> \approx (K_{stone}/2)[m_D(\Delta v)^2/2]^{1.13} = n_{ej} m_D \qquad (28)$$

In the above equation n_{ej} is some multiple of the dust particle's mass and is given by

$$n_{ej} \approx (K_{stone}/2^{2.13}) m_D^{0.13} \Delta v^{2.26} \quad . \qquad (29)$$

Assuming that $m_D \approx 10^{-6}$ kg and $\Delta v \approx 5000$ m s^{-1} give $n_{ej} \approx 61$ in (29). Thus the mass lost from the stony meteoroid by making a crater is typically many times greater than the mass of the impacting dust particle.

The amount of mass loss in ejected kilograms per second from a meteoroid of unit volume (1 m^3) is given by

$$\left.\frac{dM}{dt}\right|_{unit} = -\kappa = -(K_{stone}/2^{2.13})\frac{W_D}{\pi}\iiint w(r_1,e,I)(\Delta v)(\Delta v)^{2.26}\,dr_1 de dI \qquad (30)$$

where the extra factor Δv comes from the flux of particles hitting the unit volume and κ depends on the orbit the meteoroid is in. Also,

$$W_D = \int_0^\infty m_D^{1.13} H_m\, dm_D \quad .$$

Assume a spherical meteoroid of radius R and mass $M = 4\pi\rho R^3/3$, where ρ is the density. To get the rate of mass loss dM/dt (30) is multiplied by πR^2. It is also the case that $dM/dt = d(4\pi\rho R^3/3)/dt = 4\pi\rho R^2(dR/dt)$. Equating the two rates gives

$$\frac{dR}{dt} = -\frac{\kappa}{4\rho} = -\beta \quad . \qquad (31)$$

The quantity dR/dt will be referred to below interchangeably as the space erosion rate or abrasion rate. It is important to note that it is independent of radius R, as indicated in (31), and is constant as long as the meteoroid stays in the same orbit. It is assumed that (31) applies to all stony meteoroids regardless of composition. Stony meteorites range in

density from ~2200 kg m^{-3} to ~3900 kg m^{-3} (McCall, 1973, p. 149). A value of ρ = 2800 kg m^{-3} is adopted here.

4. Space erosion rates

Figure 8 shows the time T_{metre} to erode 1 meter of a stony meteoroid due to impacts from the combined asteroidal and core populations for the assumed abrasion model, where

$$\beta = (1 \text{ m})/T_{metre} \ , \tag{32}$$

and where the subscript is the accepted spelling of the SI unit of length. All the meteoroid orbits lie in the ecliptic; hence $I_M = 0$. The black dots show T_{metre} for meteoroids in circular orbits for semimajor axes a_M between 0.5 AU and 3.5 AU. The speediest erosion times T_{metre} occur close to the Sun, where meteoroid velocities are fast and the core N_D concentration is high (Fig. 6). A meteoroid at 0.5 AU takes 50×10^6 y to erode 1 m, while at 2 AU it is the much longer 430×10^6 y. Beyond 2.5 AU the times increase sharply, rising to $> 1000 \times 10^6$ y at 3.5 AU, which is slightly beyond the outer edge of the main belt.

The square in Fig. 8 is for a stony meteoroid with semimajor axis a_M = 2 AU and eccentricity e_M = 0.5, so that the meteoroid journeys between 1 AU to 3 AU; in other words, between the Earth and the asteroid belt. In this case $T_{metre} = 126 \times 10^6$ y. This is shorter than for a meteoroid in a circular orbit with the same semimajor axis.

The star in Fig. 8 is for a stony meteoroid with a_M = 1.75 AU and e_M = 0.714, so that it journeys between 0.6 AU and 3.5 AU. It has the quickest erosion time of all: T_{metre} = 30 × 10^6 y. It is in an orbit which takes it deep inside the core population at high velocity, as well as through the asteroidal population in the main belt; hence the short erosion time.

Iron meteoroids apparently will comminute at a rate ~270 times slower than for stony meteoroids. The estimate is made as follows. Matsui and Schultz (1984) shot ~0.15 g steel projectiles at an iron meteorite using the NASA Ames Research Center's Vertical Gun Range. They found that for speeds of ~5 km s^{-1}, the mass loss was ~2.6 times the mass of the projectile; in other words $n_{ej} \approx 2.6$. Assuming for vertical impacts

$$n_{ej} = (K_{iron}/2^{1.13})\, m_D^{0.13}\, \Delta v^{2.26} \qquad (33)$$

by analogy with (26) for m_D = 1.5 × 10^{-4} kg yields K_{iron} = 7.809 × 10^{-8} for irons, as compared to K_{stone} = 7.015 × 10^{-6} for stones.

Thus if (33) applies to iron meteoroids, then the mass loss is a factor of ~90 smaller per impact than for stony meteoroids. The density of iron meteoroids is ~7870 kg m^{-3}, a factor of ~3 larger than for stones. Hence the space erosion rate β for irons by (31) would be ~270 slower than for stones. Such slow rates are not shown in Fig. 8 and iron meteoroids would barely erode over the age of the solar system, according to the present abrasion model.

5. Space erosion rate and CRE ages of stony meteorites

How do the erosion times T_{metre} in Fig. 8 relate to the CRE ages of stones? Several simplifications are made below to give a rough answer to this question.

While Fig. 8 shows T_{metre} for two elliptical orbits and similar orbits could be calculated, only the T_{metre} for circular orbits are used here to estimate CRE ages. The rationale is that a meteoroid originating in the main belt spends little time in an elliptical orbit (Gladman et al., 1997) before impacting the Earth, offsetting the increased erosion rate.

In what follows below the cosmic ray flux is assumed to be isotropic and constant in space and time throughout the solar system. Also, meteoroids always remain spherical regardless of size as they erode away.

CRE ages are measured through the accumulation of products created from the galactic cosmic ray bombardment. The product concentration varies with depth inside a meteoroid. Neon is an example and is the only cosmic ray product examined here. Eugster et al. (2006) in their Fig. 2 show the production rates with depth of ^{21}Ne for stony spherical meteoroids for several fixed radii. For a stony spherical meteoroid whose radius remains constant, the ^{21}Ne production rate slowly increases from the meteoroid's center, and then sharply decreases as the surface is neared.

Eugster et al.'s curves can be approximated by the equations

$$P_{Ne} = [A_{Ne} + B_{Ne}(1 - e^{-d/\gamma})]e^{-d/\Gamma} \quad . \tag{34}$$

Here P_{Ne} is the production rate of ^{21}Ne in arbitrary units per 10^6 y, $B_{Ne} = 63$, and

$$A_{Ne} = 50 + 355R\, e^{-R/s} \quad , \tag{35}$$

where R is the meteoroid's radius in meters, d is the depth below the surface in meters, s = 0.333 m, and $\gamma = 0.1$ m. Also,

$$\frac{1}{\Gamma} = C_{Ne}\{1 + \tanh[h(R - R_h)]\} \quad , \tag{36}$$

where C_{Ne} = 1.111, h = 2.519, and R_h = 1.4455. The resulting curves using (34)-(36) are shown in Fig. 9 and are to be compared with Eugster et al.'s Fig. 2. The rates are computed every 0.1 m in depth. The computed points in Fig. 9 are joined by straight lines for clarity. Equations (34)-(36) and their associated constants are not based on any theory; rather, they are the result of trial-and-error and mimic Eugster et al.'s curves reasonably well for $R \geq 0.3$ m.

Suppose that a meteoroid undergoes no abrasion, so that its radius stays fixed. In this case the ^{21}Ne concentration simply increases linearly with time at any given point, and the concentration at any given instant looks the same as the production rate in Fig. 9; only the scale and units of the vertical axis change. On the other hand, for a meteoroid which does undergo space erosion, the production rate (34) holds at every instant, but the meteoroid's radius is constantly changing, resulting in curves that do not reproduce the curves in Fig. 9. What the concentration curves do look like is taken up next.

A computer program used (34)-(36) to compute the concentration inside a spherical stony meteoroid whose radius R shrinks at a constant rate due to abrasion:

$$R = R_0 - \beta t = R_0 - (1 \text{ m}/T_{metre})t \quad . \tag{37}$$

In this equation R_0 = 5 m is the initial radius at time t = 0. This value of R_0 was chosen because it is large enough to greatly shield the interior more than 3 m deep from the cosmic rays. The time step was 10^6 y.

Figure 10 shows the results for $T_{metre} = 430 \times 10^6$ y, which is the value for a stone in a circular ecliptic orbit at 2 AU (Fig. 8), and gives the fastest erosion rate in the main asteroid belt for circular orbits. The thin lines are the concentrations vs. depth for a shrinking meteoroid when the radius reaches R = 2 m, 1 m, 0.5 m, and then 0.3 m. The thick lines are the corresponding concentrations for fixed radii at these values of R; the exposure times τ_{Ne} associated with the thick lines are chosen to give concentrations which roughly agree with the thin lines at approximately half the radius of the meteoroid. The smallest value $\tau_{Ne} = 176 \times 10^6$ y in Fig. 10 occurs for stones which have radii $R > \sim 1$ m, but thereafter the values rapidly increase as the meteoroid shrinks, rising to 384×10^6 y for a 0.3 m meteoroid. It is of interest that for meteoroids with $R > \sim 1$ m the following relationship holds:

$$\tau_{Ne} \approx c_1 T_{metre} \quad , \tag{38}$$

where $c_1 \approx 0.41$. For $R < \sim 1$ m, the value of c_1 rises as the radius shrinks.

The shapes of the space erosion curves are quite different at shallow depths from those for meteoroids of fixed radii. Moving from right to left in Fig. 10, the eroding meteoroids have curves which increase or flatten out when nearing the surface, while those of fixed radii show a sharp downturn. Hence according to the present model, pristine meteoroids recovered in space will not show the downturn if they have eroded from a large body.

Meteoroids can ablate and fragment perhaps as much as 27%-99% of their mass during their passage through the Earth's atmosphere (Eugster et al. 2006, p. 833). If a meteoroid loses its outermost 0.1–0.2 m, then the part of the curve where the downturn is expected vanishes. An investigator may not realize the downturn never existed because of space erosion, and may take τ_{Ne} as the CRE age and erroneously assume that the meteoroid was liberated from deep within an asteroid a time τ_{Ne} years ago, when in fact the meteoroid could have been an independent larger body for a long time and taken longer than τ_{Ne} to drift to a resonance.

If the τ_{Ne} of eroding meteoroids are taken to be their CRE ages, then is the assumed space erosion model in any sort of disagreement with the measured CRE ages of meteorites? This question speaks to the first of the two issues raised in the Introduction.

If, as an extreme example, space erosion was so fast that the erosion τ_{Ne} values were only on the order of ~1 × 10^6 y, then a meteoroid would not have enough time to accumulate sufficient ^{21}Ne to account for the observed longer ~30 × 10^6 y ages and there would be a problem. The least upper bound on τ_{Ne} is ~176 × 10^6 y for meteoroids ~1 m in radius (Fig. 10) and larger. This limit tends to agree with what is observed: most stony

meteorites have ages < ~100 × 10^6 y. Thus it may be that space erosion sets upper limits on the CRE ages of stones which originate in the asteroid belt, but the limits are comfortably high enough to encompass the measured CRE ages, which are presumably due to Yarkovsky drift.

The time T_{metre} to erode 1 m of the surface of a hypothetical rocky and regolith-free Near-Earth asteroid (NEA) in the same orbit as the Earth is ~300 × 10^6 y. This would lead to τ_{Ne} = ~120 × 10^6 y for the assumed model. This value of T_{metre} = ~300 × 10^6 y at 1 AU is in fair agreement with one estimate of the abrasion rate of lunar rocks. Gault et al. (1972, p. 2723) find ~1mm/10^6 y for an assumed 1.5π steradian exposure for a rock on the Moon's surface. Adjusting this rate for the 4π exposure of a meteoroid gives T_{metre} = ~375 × 10^6 y, which is close to the value found here.

An improved space erosion model might increase the abrasion rate so that the τ_{Ne} actually drop into the observed range of CRE values, rather than just set upper limits. This would have implications for Yarkovsky drift. What happens in this case is discussed in the next section.

6. Yarkovsky or space erosion?

Space erosion appears to place upper limits on meteoroid CRE ages, meaning that the ages can be less, but not more. So if the Yarkovsky drift to the resonances limit stony meteoroid CRE ages to, say, the ~30 × 10^6 y observed for L chondrites (e.g., McSween, 1999, p. 246), and the abrasion least upper bound is ≤ ~176 × 10^6 y as in Fig. 10, then

there is no problem with the standard Yarkovsky scenario of how many meteoroids get their CRE ages. The ages tend to be a factor of 6 younger than the least upper bound.

But the factor of 6 is small enough to give pause. If the space erosion rates were great enough to give τ_{Ne} = ~30 × 10^6 y, and if the measured CRE ages of many stony meteorites are also ~30 × 10^6 y, then space erosion may compete with Yarkovsky.

It might even call into question whether Yarkovsky drift is the mechanism by which meteoroids reach the resonances. Meteoroids could theoretically dawdle in the asteroid belt for very long times using other mechanisms to journey to the resonances, but always turn in the observed CRE ages, thanks to space erosion.

In other words, is something wrong with Yarkovsky? Does it really operate at the expected level? If not, why not?

The ages computed here are based on a number of assumptions, and the calculated CRE ages could go up or down using a different set of assumptions. If the ages go down by a factor of ~6, then Yarkovsky could be in trouble. Hence the assumptions are worth examining to see if the factor of 6 is within reach.

Several ways to get a greater space erosion rate immediately come to mind. The most obvious is to simply raise the dust mass upper limit. Divine (1993) conveniently put the upper limit at 1 g = 10^{-3} kg, a size much larger than what is ordinarily considered "dust" (e.g., *Shirley*, 1997). The present discussion retains Divine's upper limit of 1 g; adding in bigger impactors would certainly excavate more material than considered here. This would give faster erosion, but gets into the statistics of small numbers and fracturing.

Abrasion is at one end of a continuum, with catastrophic disruption at the other end. Possibly many CRE ages might be controlled by the in-between process of spallation and abrasion (Fujiwara et al., 1977), rather than just abrasion alone. Because small impactors are more numerous than large ones, spallation will presumably be more common than catastrophic disruption, in which many fragments of all sizes are created. For instance, Matsui and Schultz (1984) found that iron meteorites sometimes fractured when hit by a 0.00015 kg (0.15 g) steel impactor. Splintering off sizeable pieces, rather than cratering, may be a way of eroding an iron meteoroid faster than the rates found here. On the other hand, Matsui and Schultz found that basaltic impactors did not create fractures at the speeds they used. Moreover, it is not clear that chunks chipped off by spallation would mimic the steady erosion that the sand-blasting by abrasion might be expected to give, unless the chunks were numerous and relatively small.

A second obvious way to get faster erosion is to tinker with Divine's populations. Grün and P. Staubach (1996) verify that Divine's five solar system dust populations fit lunar cratering, spacecraft, and zodiacal light data. But the populations, including the asteroidal and core populations considered here, are nonunique (Divine, 1993, pp. 17,032-17,033) and model-dependent (Divine, 1993 p. 17,037). Hence further information about the asteroidal population could increase or decrease the dust concentration, with a corresponding effect on CRE ages.

An alternative distribution for the asteroidal N_1 population invented for the sake of argument is shown in Fig. 5. It extends the trend in the inner solar system to 3 AU (dotted line), and then turns down and cuts off at 5 AU. The resulting T_{metre} for circular orbits are shown as the open circles in Fig. 8. No open circles are visible in the figure for

$a_M \leq 1.5$ AU because they virtually coincide with the solid black circles. But the T_{metre} are dramatically lower than from Divine's population at 2 AU and beyond, so much so that the Yarkovsky interpretation for stones might be in trouble if this or a similar alternative distribution were to hold.

However, Divine (1993, p. 17,037) states that a dust distribution which continues the trend in the inner solar system would make too large a contribution to the zodiacal light for his assumed geometric albedo of 0.01. Hence adopting the alternative distribution may not be viable. Further, a more accurate distribution than Divine's might just as well decrease the dust concentration as increase it.

There is also the question as to whether the dust populations have stayed constant over time. It is assumed here that they have stayed the same over hundreds of millions of years. However, the dust populations have presumably varied over geologic time, as reflected in the dust influx to the Earth (e.g., Gault et al., 1972; Peucker-Ehrenbrink, 2001; Mukhopadhyay et al., 2001). The present influx may be twice the average influx over the past 70×10^6 y (Farley, 2001, p. 1194), so that the abrasion rates may be smaller than found above. On the other hand, collisions in the asteroid belt may yield temporary local dense concentrations of dust which would accelerate space erosion there.

Further, the present model assumes a constant flux over geologic time for the galactic cosmic rays. This may not be the case (e.g., Eugster et al., 2006).

A final obvious way to get a greater abrasion rate is to assume more material is lifted off from microcratering than given by (29) and (33). Low temperatures in the asteroid belt may make the rock more brittle, thus increasing the mass loss beyond what is given by (29) and (33).

So: can the model be reasonably altered enough to accommodate the factor of ~6 and cast doubt on Yarkovsky? As shown above, arguments can be adduced to either increase or decrease the space erosion rate. At the present time the question remains open.

7. Discussion

Only ^{21}Ne concentrations are examined here in relation to CRE ages. It was more or less assumed that τ_{Ne} equates with CRE age. Neither other cosmic ray products, such as ^{3}He, nor tracks are considered in relation to the space erosion model.

All rocky surfaces in the solar system which remain free of regolith may have the upper limit on their CRE ages controlled by space erosion. The particular limits depend upon the dusty environment they find themselves in, as shown in Fig. 8. Erosion rates inside 1 AU are rapid. Such fast erosion might have implications for the CRE ages of regolith-free Near-Earth Asteroids (NEAs) and any meteorites which originate from them (Morbidelli et al., 2006). Pristine samples returned from an NEA may not show the downturn in the ^{21}Ne concentration as the surface is neared (Fig. 10).

The presence of regolith could impede the abrasion of the monolithic rock underneath by being thick enough to intercept the dust bombardment, but perhaps still be thin enough to allow the cosmic rays to penetrate the rubble and age what is below. Presumably meteoroids and the smallest asteroids are regolith-free.

On the issue of whether space erosion or Yarkovsky controls CRE ages, the Yarkovsky effects depend on principal axis rotation. The diurnal Yarkovsky effect

depends on the meteoroid's sense of rotation, increasing the semimajor axis for prograde rotation and decreasing it for retrograde rotation. The YORP effect (e.g., Paddack, 1969; Paddack and Rhee, 1975; Rubincam, 2000; Bottke et al., 2002; Vokrouhlicky et al., 2006; Statler, 2009) or collisions might change the spin axis orientation enough to lessen diurnal Yarkovsky's effectiveness by a random walk, but the seasonal Yarkovsky effect (Rubincam, 1987, 1995) will still be operative regardless of where the spin axis is, unless the meteoroid tumbles most of the time, which seems unlikely.

At the young end of the CRE age distribution, it is hard to see how space erosion could explain the shortest observed ages of $\leq \sim 10^6$ y regardless of how much the abrasion rate is increased. (Yarkovsky also has trouble with such young ages; Morbidelli et al., 2006). Moreover, an improved model might just as well lower abrasion rates as raise them. Further research is needed to see whether space erosion casts doubt on the hypothesis that Yarkovsky drift to the resonances controls many meteorite CRE ages.

At the other end of the CRE age distribution, the aubrites also pose a problem for space erosion controlling stony CRE ages. They are fragile but tend to have long ages. A possible way to resolve the problem is if the aubrite parent body is in an orbit inclined to the ecliptic, which would lessen collisional encounters (McSween, 1999, p. 247). Inclined orbits are not considered here.

The iron meteoroids have the oldest CRE ages and present another possible obstacle. Their abrasion rates appear to be so slow that they undergo little erosion (Matsui and Schultz, 1984 and section 4 above), so that their CRE ages might be controlled by Yarkovsky. Thus there would be two separate explanations as to how

meteorites get their CRE ages: space erosion for stones and Yarkovsky for irons, rather than one elegant unifying explanation.

A potential way around the iron problem is the combined abrasion and fracturing mentioned in section 6. Irons might "erode" mainly by spallation (Matsui and Schultz, 1984), which might explain their CRE ages, rather than Yarkovsky.

The results above cast some doubt on the Yarkovsky interpretation of meteorite CRE ages. More research is needed to clarify the issue.

Appendix

Divine (1993) gives the correct expressions for the dust particle speeds v_ϕ, v_r, v_s, and v_x, v_y, v_z, but does not derive them. The purpose of this appendix is to outline their derivation, in order to save readers time when it comes to verifying the equations for themselves.

The velocity of the dust particle is given by (19). The speed v_ϕ is most easily found first. By Kepler's law $r^2(d\phi/dt) = [GM_S\, a(1 - e^2)]^{1/2}$, where ϕ is the angle in the orbital plane. Using the relation $r_1 = a(1 - e)$ to eliminate semimajor axis a yields $v_\phi = r(d\phi/dt) = +[GM_S r_1(1+e)/r^2]^{1/2}$, which agrees with (24). The radial speed v_r can then be found from $v_r^2 = \pm(v^2 - v_\phi^2)^{1/2}$ and the energy relation $v^2 = GM_S\,[(2/r) - (1/a)]$ after once again eliminating a, yielding (23).

Finding v_s is harder work. By (1)-(2) and (19)

$v_\phi(\hat{\mathbf{n}} \times \hat{\mathbf{r}}) \cdot \hat{\mathbf{x}}$

$= -v_\phi [(z/r) \sin I \cos \Omega + (y/r) \cos I]$, (A1)

$v_\phi(\hat{\mathbf{n}} \times \hat{\mathbf{r}}) \cdot \hat{\mathbf{y}}$

$= v_\phi [(x/r) \cos I - (z/r) \sin I \sin \Omega]$, (A2)

$v_s = v_\phi(\hat{\mathbf{n}} \times \hat{\mathbf{r}}) \cdot \hat{\mathbf{z}}$

$= v_\phi [(y/r) \sin I \sin \Omega + (x/r) \sin I \cos \Omega]$ (A3)

Also, because $\hat{\mathbf{n}}$ is perpendicular to $\hat{\mathbf{r}}$

$\hat{\mathbf{n}} \cdot \hat{\mathbf{r}} = (x/r) \sin I \sin \Omega - (y/r) \sin I \cos \Omega + (z/r) \cos I = 0$ (A4)

Squaring (A3) results in a term containing $2xy$ times some other factors. Squaring (A4) also contains in the same $2xy$ term. Using the square of (A4) to eliminate the $2xy$ term in v_s^2 ultimately results in the desired result $v_s^2 = v_\phi^2(\cos^2 \lambda - \cos^2 I)$, which is the square of (25), after using $\sin \lambda = z/r$ to get rid of z. This completes finding v_ϕ, v_r, and v_s.

The expressions for v_x, v_y, and v_z will be found next. The velocity vector is given by **(19).** The first term on the right-hand side of (20), (21), and (22) is clearly the Cartesian component of $v_r\hat{\mathbf{r}}$; it remains to find the Cartesian components of $v_\phi(\hat{\mathbf{n}} \times \hat{\mathbf{r}})$.

Rearranging (A4) results in $\sin I \sin \Omega = (y/x) \sin I \cos \Omega - (z/x) \cos I$. Substituting this in (A3) and rearranging gives

$$\sin I \cos \Omega = \frac{rx}{x^2 + y^2}\left(\frac{v_s}{v_\phi} + \frac{yz \cos I}{rx}\right)$$

Substituting this in (A1) ultimately gives the second term on the right-hand side of (20). A similar derivation gives the second term on the right-hand side of (21). The speed v_s has already been found, which is the second term on the right-hand side of (22).

Acknowledgment

I thank Susan Poulose and Susan Fricke for excellent programming. NASA Advanced Exploration Systems (AES) supported this work.

References

Afonso, G. B., Gomes, R. S., Florczak, M. A., 1995. Asteroid fragments in Earth-crossing orbits. Planet. Space Sci. 43, 787-795. doi:10.1016/0032-0633(94)00171-M.

Beckmann, P., 1973. Orthogonal Polynomials for Engineers and Physicists. Golem Press, Boulder, CO.

Blanco, V. M., McCuskey, S. W., 1961. Basic Physics of the Solar System. Addison-Wesley, Reading, MA.

Bottke, W. F., Rubincam, D. P., Burns, J. A., 2000. Dynamical evolution of main belt meteoroids:numerical simulations incorporating planetary perturbations and Yarkovsky thermal forces. Icarus 145. 301-331. doi: 10.1006/icar.2000.6361

Bottke, W. F., Vokrouhlicky, D., Rubincam, D. P., Broz, M., 2002. Dynamical evolution of asteroids and meteoroids using the Yarkovsky effect. In: Bottke, W. F., Cellino, A., Paolicchi, P., Binzel, R. (Eds.), Asteroids III, Univ. of Arizona Press, Tucson, AZ, pp. 395-408.

Buchwald, V. F., 1975. Handbook of Iron Meteorites. Univ. of California Press, Berkeley, CA.

Divine, N., 1993. Five populations of interplanetary meteoroids. J. Geophys. Res. 98, 17,029-17,048. doi: 10.1029/93JE01203.

Eugster, O., Herzog, G. F., Marti, K., Caffee, M. W., 2006. Irradiation records, cosmic-ray exposure ages, and transfer times of meteorites. In: Lauretta, D. S., McSween, H. Y. (Eds.), Meteorites and the Early Solar System II, Univ. of Arizonz Press, Tucson, AZ, pp. 829-851.

Farinella, P., Vokrouhlicky, D., 1999. Semimajor axis mobility of asteroidal fragments. Science 283, 1507-1510. doi: 10.1126/science.283.5407.1507.

Farley, K. A., 2001. Extraterrestrial helium in seafloor sediments: Identification, characteristics, and accretion rate over geologic time. In: Peucker-Ehrenbrink, B., Schmitz, B. (Ed.s), Accretion of Extraterrestrial Matter Throughout Earth's History. Kluwer Academic/Plenum Publishers, New York, pp. 179-204.

Fisher, D. E., 1961. Space erosion of the Grant meteorite. J. Geophys. Res. 66, 1509-1511. doi: 10.1029/JZ066i005p01509.

Fujiwara, A., Kamimoto, G., Tsukamoto, A., 1977. Destruction of basaltic bodies by high-velocity impact. Icarus 31, 277-288. doi: 10.1016/0019-1035(77)90038-0.

Gault, D. E., Hörz, F., Hartung, J. B., 1972. Effects of microcratering on the lunar surface. Proc. Third Lunar Sci. Conf., Vol. 3, pp. 2713-2734.

Gladman, B. J., Migliorini, F., Morbidelli, A., Zappala, V., Michel, P., Cellino, A., Froeschle, C., Levison, H. F., Bailey, M., and Duncan, M., 1997. Dynamical lifetimes of objects injected into asteroid belt resonances. Science 277, 197-201. doi: 10.1126/science.277.5323.197.

Greenberg, R., and Nolan, M. C., 1989. Delivery of asteroids and meteorites to the inner solar system. In Binzel, R. P., Gehrels, T., Matthews, M. S. (Ed.s), Asteroids II, Univ. of Arizona Press, Tucson, AZ, 778-804.

Grün, M. J., Staubach, P., 1996. Dynamic populations of dust in interplanetary space. In: Gustafson, B. A. S., and Horner, M. S. (Ed.s), Physics, Chemistry, and Dynamics of Interplanetary Dust. ASP Conference Series, vol. 104, Astron. Soc. Pacific, pp. 15-18.

Hughes, D. W., 1982. Meteorite erosion and cosmic ray variation. Nature 295, 279-280. doi: 10.1038/295279a0.

Matney, M. J., Kessler D. J., 1996. A reformulation of Divine's interplanetary model. In: Gustafson, B. A. S., and Horner, M. S. (Ed.s), Physics, Chemistry, and Dynamics of Interplanetary Dust. ASP Conference Series, vol. 104, Astron. Soc. Pacific, pp. **15-18.**

Matsui, T., Schultz, P. H., 1984. On the brittle-ductile behavior of iron meteorites: new experimental constraints. *LPSC*, *XV*, 519-520.

McCall, G. J. H., 1973. Meteorites and Their Origin. Wiley, New York.

McSween, H. Y., 1999. Meteorites and Their Parent Bodies, 2nd. ed., Cambridge Univ. Pr., New York.

Morbidelli, A., Gounelle, Levison, H. F., Bottke, W. F., 2006. Formation of the binary near-Earth object 1996 FG_3: Can binary NEOs be the source of short-CRE meteorites? Meteoritics Plan. Sci. 41, 875-887.

Mukhopadhyay, S., Farley, K. A., Montanari, A., 2001. A 35 Myr record of helium in pelagic limestones from Italy: Implications for interplanetary dust accretion from the early Maastrichtian to the middle Eocene. Geochim. Cosmochim. Acta 65, 653-669. doi:10.1016/S0016-7037(00)00555-X.

Nakamura, A. M., Fijiwara, A., and Kadono, T., 1994. Velocity of finer fragments from impact. Planet. Space. Sci. 42, 1043-1052. doi: 10.1016/0032-0633(94)90005-1.

Norton, O. R., 1994. Rocks from Space. Mountain Press, Missoula, Montana.

Nunes, J. A., 1994. In memoriam: T. Neil Divine (1939-1994). Icarus 109, 2. doi: 10.1006/icar.1994.1073.

O'Keefe, J. A., 1976. Tektites and Their Origin. Elsevier, New York.

Öpik, E. J., 1951. Collision probabilities with the planets and the distribution of interplanetary matter. Proc. R. Irish Acad. 54A, 165-199.

Paddack, S. J., 1969. Rotational bursting of small celestial bodies: Effects of radiation pressure. J. Geophys. Res. 74, 4379-4381. doi: 10.1029/JB074i017p04379.

Paddack, S. J., Rhee, J. W., 1975. Rotational bursting of interplanetary dust particles. Geophys. Res. Lett. 2, 365-367. doi: 10.1029/GL002i009p00365.

Peterson, C., 1976. A source mechanism for meteorites controlled by the Yarkovsky effect. Icarus 29, 91-111. doi: 10.1016/0019-1035(76)90105-6.

Peucker-Erenbrink, B., 2001. Iridium and osmium as tracers of extraterrestrial matter in marine sediments. In: Peucker-Ehrenbrink, B., Schmitz, B. (Ed.s), Accretion of Extraterrestrial Matter Throughout Earth's History. Kluwer Academic/Plenum Publishers, New York, pp. 163-178.

Rubincam, D. P. 1987. LAGEOS orbit decay due to infrared radiation from earth. J. Geophys. Res. 92, 1287-1294. doi: 10.1029/JB092iB02p01287.

Rubincam, D. P., 1995. Asteroid orbit evolution due to thermal drag. J. Geophys. Res. 100, 1585-1594. doi: 10.1029/94JE02411.

Rubincam, D. P., 2000. Radiative spin-up and spin-down of small asteroids. Icarus 148, 2-11. doi: 10.1006/icar.2000.6485.

Selby, S. M., 1974. CRC Standard Mathematical Tables, 22nd ed., CRC Press, Cleveland, OH.

Shaeffer, O. A., Nagel, K., Fechtig, H., Neukum, G., 1981. Space erosion of meteorites and the secular variation of cosmic rays (over 10^9 years). Planet. Space Sci. 29, 1109-1118. doi: 10.1016/0032-0633(81)90010-6.

Shirley, J. H., 1997. Dust. In: Shirley, J. H., Fairbridge R. W. (Ed.s), Encyclopedia of Planetary Sciences, Chapman & Hall, New York, pp. 189-192.

Statler, T. S., 2009. Extreme sensitivity of the YORP effect to small-scale topography. Icarus 202, 502-513. doi: 10.1016/j.icarus.2009.03.003.

Vokrouhlicky, D., Nesvorny, D., Bottke, W. F., 2006. Seculat spin dynamics of inner main-belt asteroids. Icarus 184, 1-28. doi: 10.1016/j.icarus.2006.04.007.

Welten, K. C., Nishiizumi, K., Caffee, M. W., Schultz, L., 2001. Update on exposure ages of diogenites: The impact and evidence of space erosion and/or collisional disruption of stony meteoroids. Meteoritics & Planet. Sci. 36, supplement, A223.

Whipple, F. L., 1962. Meteorite erosion in space. Astron. J. 67, 285. doi: 10.1086/108864.

Whipple, F. L., Fireman, E. L., 1959. Calculation of erosion in space from the cosmic-ray exposure ages of meteorites. Nature 183, 1315. doi:10.1038/1831315a0.

Wieler, R., Graf, T., 2001. Cosmic ray exposure: History of meteorites. In: Peucker-Ehrenbrink, B., Schmitz, B. (Ed.s), Accretion of Extraterrestrial Matter Throughout Earth's History. Kluwer Academic/Plenum Publishers, New York, pp. 221-240.

Wisdom, J., 1987. Chaotic dynamics in the solar system. Icarus 72, 241-275. doi: 10.1016/0019-1035(87)90175-8.

Wood, J. A., 1968. Meteorites and the Origin of the Planets. McGraw-Hill, New York.

Table 1. Constants used in p_I, which has the piecewise form $p_I = c + b \cos I$ in the various intervals for I.

I	c	b
0-10°	0.0	−0.173725
10-20°	−34.441201	37.741467
20-30°	−0.0862278	10.082696
30-40°	−8.449943	1.321211
45-60°	−0.173725	0.347451
60-180°	0.0	0.0

Table 2. Constants A_j used for p_e, where $p_e = \Sigma A_j e^j$ over the entire range of eccentricity 0-1.

j	A_j
0	0.577483
1	16.491390
2	25.200077
3	−1110.493161
4	6500.064217
5	−19912.701496
6	37816.824484
7	−46200.552344
8	35329.116437
9	−15343.317775
10	2878.802491

Table 3. Constants used for N_1 for the asteroidal and core populations in the r_1 intervals listed. Both have the piecewise form $N_1 = Cr_1^{\alpha}$.

r_1 (AU)	α	$\log_{10} C$
Asteroidal		
0.1-1.1	3.65185	−21.134
1.1-2.2	1.66429	−17.331
2.2-2.5	0.00010	−16.830
2.5-20.0	−3.51017	−16.830
Core		
0.01-0.1	−1.3	−16.980
0.1-1.0	−1.3	−18.280
1.0-2.0	−1.3	−19.580
2.0-4.0	−16.706	−19.971

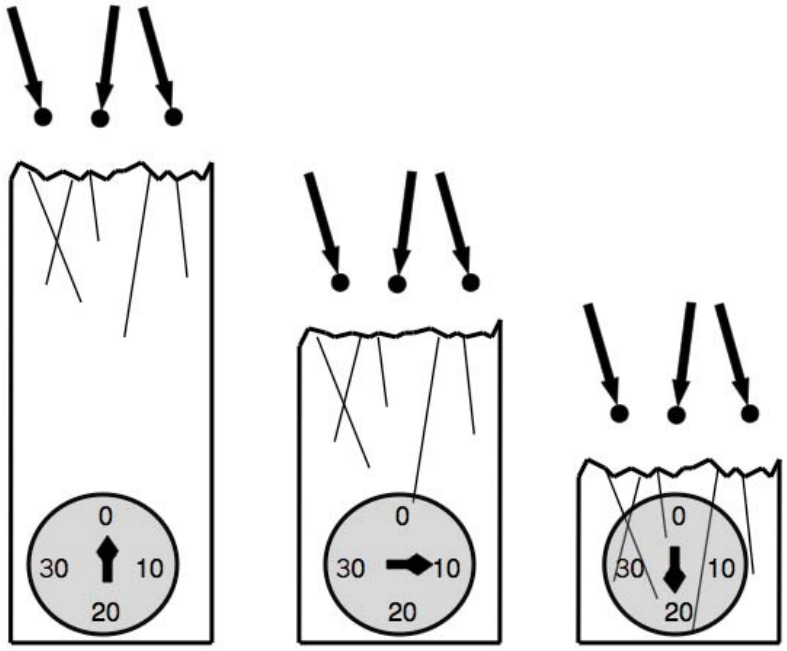

Fig. 1. The space erosion scenario. A clock inside a meteoroid measures the cosmic ray exposure (CRE) age. Left: The CRE clock is initially too deeply buried to be reached by cosmic rays (thin lines) and the clock face reads zero. Center: Once the surface erodes enough from dust impacts (dots) so that it is about a meter from the clock, the clock starts ticking. Right: The CRE clock records its maximum age when the eroding surface reaches it.

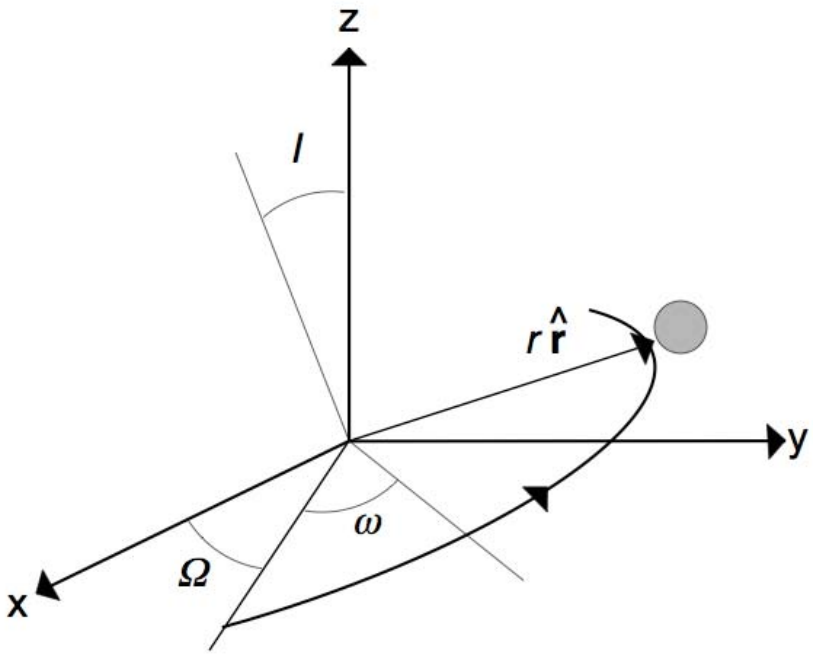

Fig. 2. Geometry of a dust particle orbit. The unit vectors $\hat{\mathbf{x}}$, $\hat{\mathbf{y}}$, and $\hat{\mathbf{z}}$ form a right-handed coordinate system, with $\hat{\mathbf{z}}$ being normal to the ecliptic. The unit vector $\hat{\mathbf{n}}$ is normal to the orbital plane and makes an angle I with $\hat{\mathbf{z}}$. The ascending node of the orbital plane makes an angle Ω in the ecliptic. The perihelion distance is r_1. The particle is at $r\hat{\mathbf{r}}$, where $\hat{\mathbf{r}}$ is the unit position vector and r is the distance from the Sun.

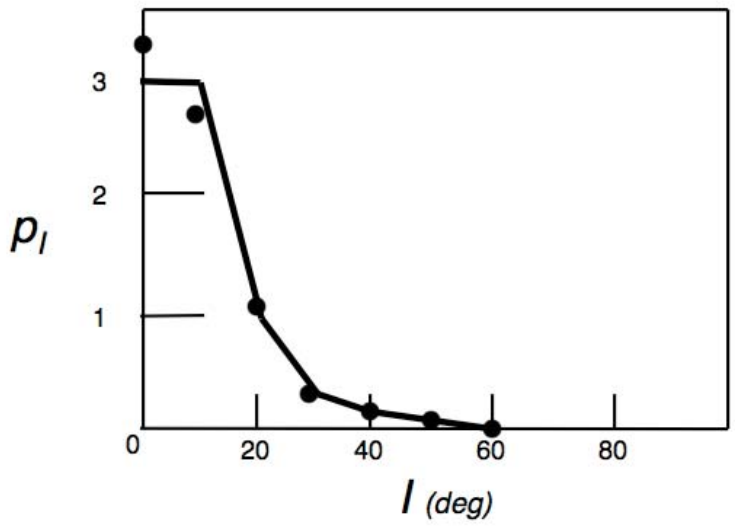

Fig. 3. Graph of p_I vs. I, which is the same for the core and asteroidal populations. Divine's (1993) piecewise function of the form $c + bI$ is given by the solid lines. The dots show the values of the piecewise function used here, which has the form $c + b\cos I$.

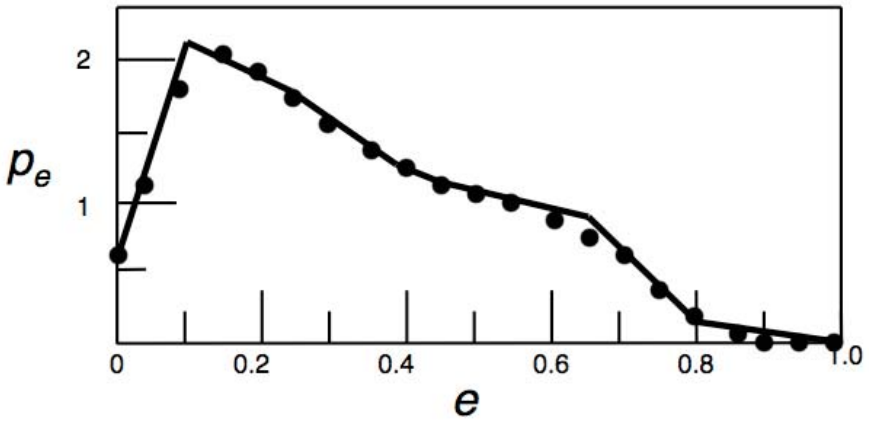

Fig. 4. Graph of p_e vs. e, which is the same for the core and asteroidal populations. Divine's (1993) piecewise function is given by the solid lines. The dots show the values of the polynomial function in e used here, as given by (17).

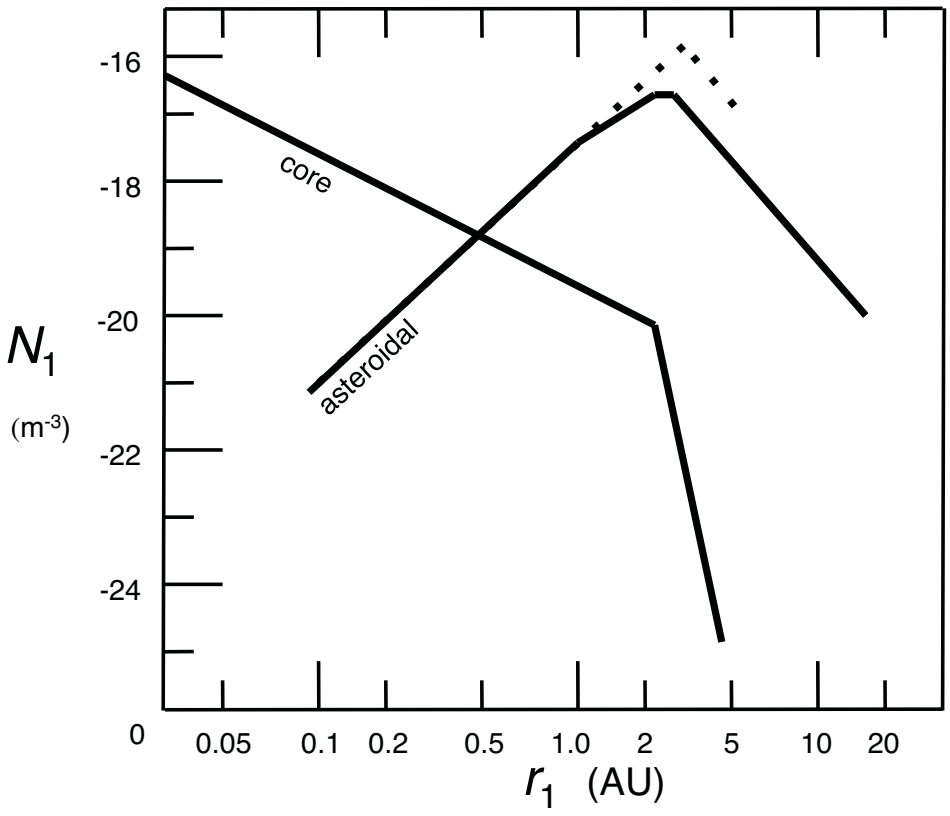

Fig. 5. The solid lines are Divine's (1993) dust number concentration N_1 for the core and asteroidal populations as a function of perihelion distance r_1 from the Sun. The dotted line between 1 AU and 5 AU is an alternative concentration to Divine's: it continues Divine's slope, followed by a downturn and cut-off at 5 AU.

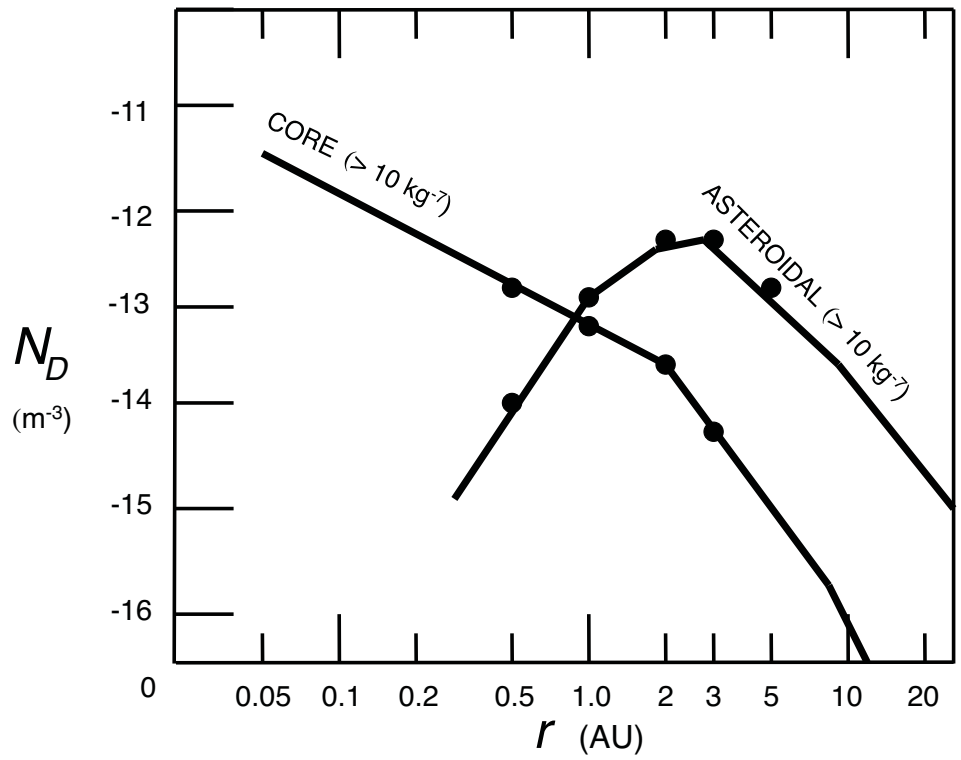

Fig. 6. Dust number concentration N_D in the ecliptic as a function of distance r from the Sun for both the core and asteroidal populations for dust particles with masses > 10^{-7} kg. Divine's (1993) concentrations are given by the solid lines. The dots are the values computed as described in section 2 for 0.5 AU ≤ r ≤ 5 AU.

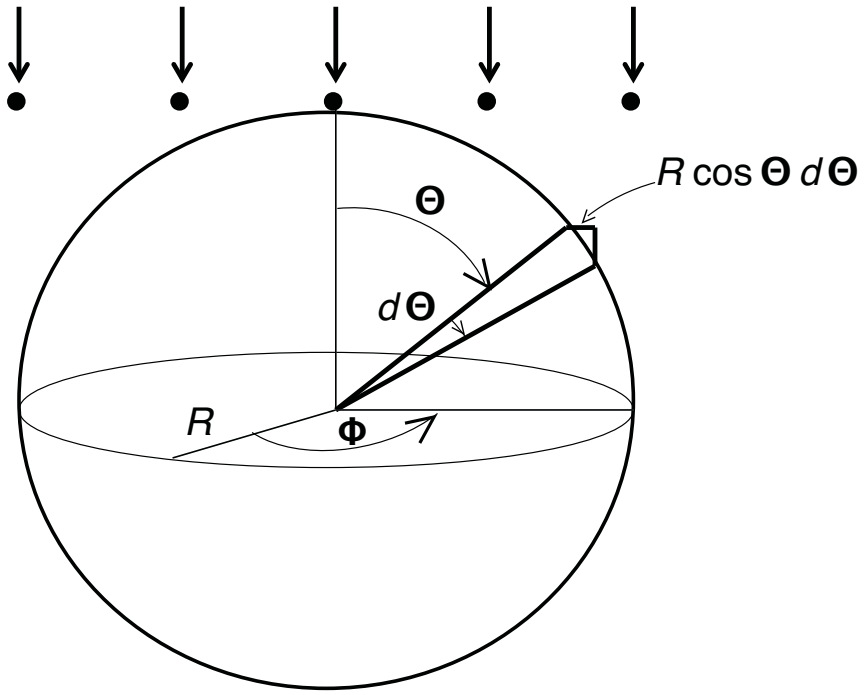

Fig. 7. Geometry of dust particles impinging on a spherical meteoroid from a particular direction. The dust particles (black dots) are spread evenly over the cross-sectional area πR^2 seen by the particles, where R is the meteoroid's radius. Φ the longitude on the meteoroid, while Θ is the colatitude. A particle impacting on the annulus of radius $R\sin\Theta$ and width $R\cos\Theta d\Theta$ ejects mass which is proportional $\cos^2\Theta$.

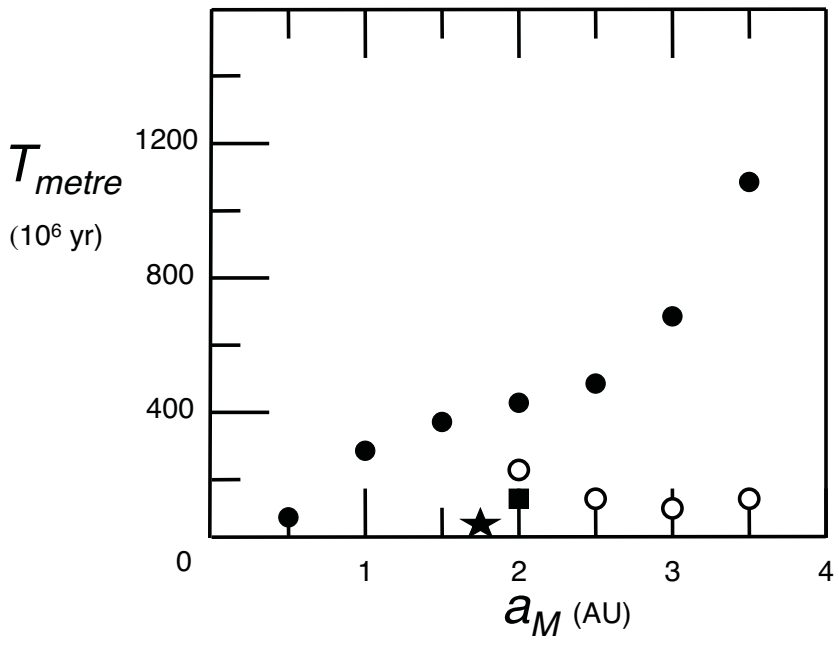

Fig. 8. The time T_{metre} required to erode a meter of a stony meteoroid from dust impacts as a function of a meteoroid's orbital semimajor axis a_M for $I = 0°$. The solid circles are for circular orbits, the square gives T_{metre} for $a_M = 2$ AU and $e_M = 0.5$, and the star gives the value for $a_M = 1.75$ AU and $e_M = 0.714$, all using Divine's populations. The open circles give the values for circular orbits using Divine's core population plus the alternative asteroidal population shown in Fig. 5.

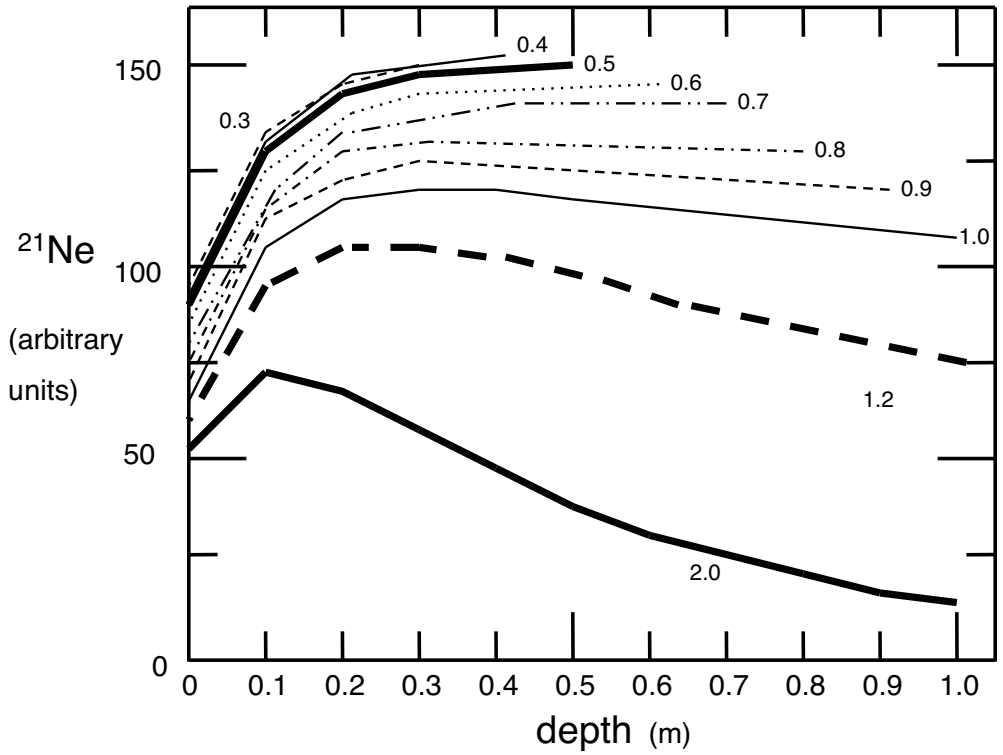

Fig. 9. The ^{21}Ne production rates from cosmic ray bombardment as function of depth inside spherical meteoroids of fixed radii. The rates are in arbitrary units, computed using (34)-(36). The meteoroid radii range from 0.3 m to 2 m. The rates are computed every 0.1 m. The computed points are joined by straight lines for clarity. This figure is to be compared to Fig. 2 of Eugster et al. (2006).

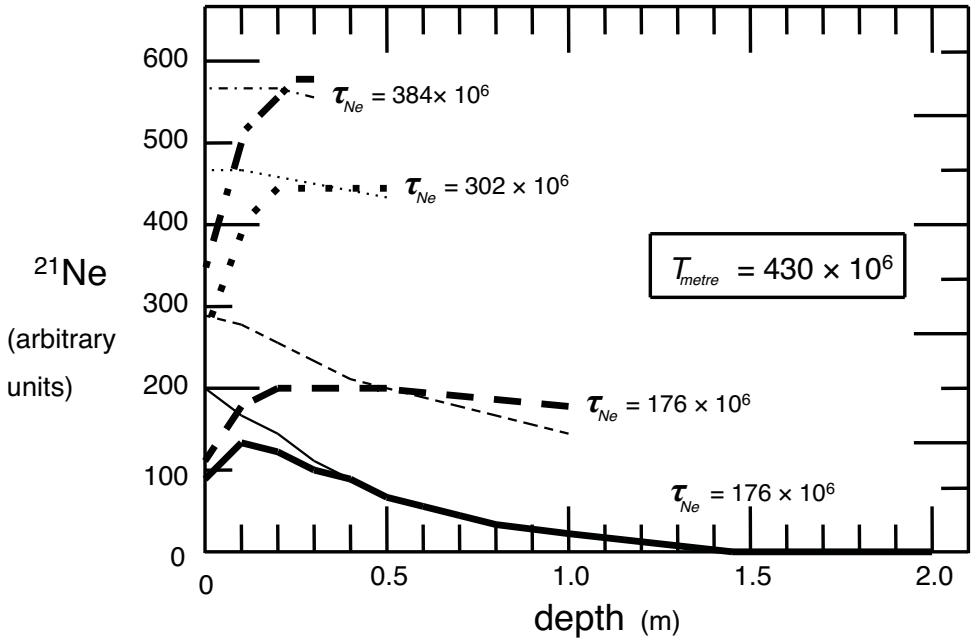

Fig. 10. The ^{21}Ne concentrations from cosmic ray bombardment as function of depth inside a spherical meteoroid in a circular orbit at 2 AU undergoing space erosion, for an initial radius of 5 m and $T_{metre} = 430 \times 10^6$ y. The concentrations are in arbitrary units, and are computed every 0.1 m. The computed points are joined by straight lines for clarity. The thin lines are for when a shrinking meteoroid's radius reaches 2 m, 1 m, 0.5 m, and 0.3m. The thick lines are corresponding concentrations for meteoroids whose sizes remain constant at these values of radius. The exposure times τ_{Ne} associated with the thick lines are chosen to give concentrations which roughly agree with the thin ones at approximately half the radius. The eroding meteoroid does not show a downturn in concentration as the surface is neared, but a non-eroding meteoroid would.